Catalysis Letters Vol. 99, Nos. 3–4, Feburary 2005 (© 2005)
DOI: 10.1007/s10562-005-2108-6

Catalytic combustion of methane on novel catalysts derived from Cu–Mg/Al-hydrotalcites

Zheng Jiang,[1] Zhengping Hao,[1,*] Junjie Yu,[1] Hongxia Hou,[1] Chun Hu[1] and Jixin Su[2]

[1]*Research Center for Eco-Environmental Sciences, Chinese Academy of Sciences, Beijing 100085, P.R. China*
[2]*Environmental Sciences and Engineering School, Shandong University, Ji'nan, 250100, P.R. China*

Received 17 May 2004; accepted 5 October 2004

Novel Cu–Mg/Al mixed oxides (designated as i-CMAO-800) were prepared by calcinations of Cu–Mg/Al-hydrotalcites [$(Cu^{2+} + Mg^{2+})/Al^{3+} = 3$] at 800 °C. Their performance for the catalytic combustion of methane was investigated. The oxides and their precursors were characterized by XRD, TG-DSC, TPR and N_2 adsorption/desorption techniques. The results showed that BET surface areas and the stability of the resultant oxides were greatly influenced by the copper contents in hydrotalcite precursors, bringing about difference in their activities for methane catalytic combustion. XRD results indicated that Cu was highly dispersed in hydrotalcite precursors in case of low copper contents, (Cu 40 wt%). For higher Cu contents, $Cu(OH)_2$ was formed, and, consequently, a separate phase of CuO was detected in the oxide catalysts after calcination. As indicated by the TG-DSC results, different decomposition behaviors were observed for various hydrotalcites. Thermal calcination promoted the formation of copper aluminates and segregation of CuO from the bulk phases. TPR results showed 15CMAO-800 has the highest reduction rate, and the catalytic activities of iCMAO-800 mixed oxides depend on both the reduction rates and the amounts of copper ions in mixed oxides. The catalyst 15-CMAO-800 showed the best performance.

KEY WORDS: methane catalytic combustion; copper-containing oxides; hydrotalcites.

1. Introduction

Hydrotalcite-like compounds (HTLCs), which are also called anionic clays or Layered Double Hydroxides (LDHs), can be formulated by $M^{II}_{1-x}M^{III}_{x}(OH)_2(A^{n-})_{x/n} \cdot yH_2O$, where $M^{II} = Cu^{2+}$, Ni^{2+}, Co^{2+}, Zn^{2+}, and Mn^{2+} ; $M^{III} = Al^{3+}$, Fe^{3+}, Cr^{3+}, Ga^{3+}, In^{3+}, V^{3+}, Ru^{3+}, and Rh^{3+}, and A^{n-} are anions existing in layers [1–5]. Hydrotalcite-like anionic clays are good function materials used as adsorbents, ion exchangers, base catalysts, and potential precursors of mixed oxides for catalytic application, because these compounds can be easily converted into well-mixed oxides via calcination [1–4] In recent years, some new hydrotalcites with substitution of Mg^{2+} by Zr^{4+}, Ti^{4+} or Sn^{4+} etc, have been synthesized [1,3,6–8]. The interesting properties of these materials depend on their specific brucite-like octahedral layered structures. Transition metal oxides derived from hydrotalcite anionic clay precursors have been widely used as heterogeneous catalysts because of their highly uniform distribution of cations, their fairly high surface areas and their great potential to be modified to obtain good catalytic properties [1,3]. HTLCs have been extensively investigated for the development of new environmental friendly catalytic systems, such as steam reforming of methanol for the production of CO-free hydrogen (OSRM), selective catalytic reduction of NO_x (SCR) and selective catalytic oxidization (SCO) of ammonia on Cu-based mixed oxides derived from Cu-containing hydrotalcites [9–12]. However, no application of these kinds of materials to the catalytic combustion of natural gas has been reported.

It is well known that catalytic combustion of natural gas is an environment friendly and energy-efficient technology for power and heat generation with ultra-low emission of NO_x, CO, and unburned hydrocarbons. Nevertheless, there remains a major problem for the application of catalytic combustion unsettled, namely, the scarcity of robust and stable catalysts for catalytic combustion under severe hydrothermal conditions [13, 14]. Extensive efforts have been made to develop suitable catalysts and overcome these key obstacles for commercial applications. Generally, supported noble metal oxides, such as palladium and platinum oxides, are excellent catalysts below 800 °C, however they are very expensive and prone to coarsening and deactivation above 800 °C, since they suffer the growth of larger grains by high-temperature sintering [l5,16]. Copper-based oxide catalysts have comparatively good activities and relatively low costs. Unfortunately, sintering and evaporation of Cu in both bulk and supported Cu-containing oxides restricted the application of copper catalysts for the catalytic combustion of natural gas [17,18]. In view of their excellent properties of oxides derived from hydrotalcites, the CuMgAlO oxides derived from HTLCs are probably good alternatives of the conventional Cu-based catalysts in catalytic combustion of natural gas, because Cu can be highly dispersed and stabilized by Mg/Al oxides.

*To whom correspondence should be addressed.
E-mail: zpinghao@mail.rcees.ac.cn

In the present work, Cu-based oxide catalysts have been prepared from Cu-containing hydrotalcites and their performance in catalytic combustion of methane has been studied. It is well known that the formation of good HTLCs structure requires an optimum M^{2+}/M^{3+} ratio of approximately 3, but it is difficult to synthesize pure Cu-containing binary hydrotalcites because of the Jahn–Teller distortion. Fortunately, copper can be incorporated in the HTLC matrix in the presence of other cations to form ternary hydrotalcites [1,10]. We have succeeded to prepare a series of CuMgAl-mixed oxides by calcining their hydrotalcite precursors (HTLCs) with $(Cu^{2+} + Mg^{2+})/Al^{3+}$ in a molar ratio of 3. These CuMgAlO oxides and their precursors were characterized by using XRD and TG-DSC techniques. The reduction behaviors of the resultant oxides were studied by temperature-programmed reduction (TPR) technique.

2. Experimentals

2.1. Catalyst preparation

Seven copper-magnesium/aluminium hydrotalcites (Cu–Mg/Al-HTLCs, weight percents of CuO in resultant oxides are 0, 5, 10, 15, 20, 30, 40 wt% respectively) with $(Cu^{2+} + Mg^{2+})/Al^{3+} = 3$ were synthesized using the aqueous precipitation method. In brief, they were obtained by co-precipitation from two aqueous solutions A and B. Solution A contains stoichiometric amounts of $Cu(NO_3)_2 \cdot 6H_2O$, $Mg(NO_3) \cdot 6H_2O$ and $Al(NO_3)_3 \cdot 9H_2O$ in doubly distilled water, whereas solution B is a freshly prepared KOH solution. Solutions A and B were simultaneously dropped into 150 mL doubly distilled water within 1 h under vigorously stirring, and the solution pH was kept at 9 ± 0.5. The resultant gel was aged with stirring for 4 h. Then the precipitates were subsequently washed and filtered several times to remove K^+ and other residual anions. Finally, the filtration cakes were dried in oven at 110 °C for 48 h to obtain Cu–Mg/Al-HTLCs (designated as iCMA-HTLC). The Cu–Mg/Al mixed oxides catalysts were obtained by calcining Cu–Mg/Al-HTLCs at 800 °C for 5 h. The Cu–Mg/Al mixed oxides are denoted as i-CMAO-800, where i ($0 \leq i \leq 40$) represents the weight percent of CuO in the mixed oxides. For example, 5CMAO-800 refers to the catalyst with CuO 5 wt% and the calcinations temperature is 800 °C, and Mg/Al oxides calcined at different temperatures are denoted as 0CMAO-800.

Platinum/alumina catalyst (1 wt% Pt loading) was prepared by the impregnation method. Alumina support (pre-calcined at 800 °C/4 h) was suspended in an aqueous solution of choloriplatinic acid and oxalic acid ($C_2H_2O_4$). After evaporation and calcinations at 500 °C, the sample was reduced with H_2 at 500 °C.

2.2. Catalyst characterization

2.2.1. X-ray diffraction

The crystal structure of the prepared materials was determined by XRD continuous scan analysis using a Japan Rigaku, D/max-RB X-Ray Diffractometer, employing CuK_α radiation ($\lambda = 1.5418$ Å), Ni filter, scan speed 4/min, count Mode CPS, voltage 40 kV, current 120 mA.

2.2.2. Surface area measurement

The specific surface areas of the solid samples were measured by N_2 adsorption at 77 K in a Quantachrome NOVA 1200 Sorptomatic apparatus.

2.2.3. TG-DSC

The thermal decomposition and stability of iCMA-HTLC samples (40 mg) were studied by thermogravimetry and differential scanning calorimetry (TG and DSC, Seteram, Labsys^{TM}) with high-purity N_2 as the carrier gas at a heating rate of 10 °C/min. Al_2O_3 crucibles were used.

2.2.4. TPR

Temperature-programmed reduction (TPR) was performed for all the iCMAO-800 catalysts on a conventional TPR apparatus equipped with a thermal conductivity detector (TCD). Catalyst samples (50 mg each), were inserted in a quartz reactor land sandwiched between two quartz wool plugs. Prior to each TPR run, the catalyst was heated up to 500 °C under an O_2 flow (40 mL/min). After a 30-min pretreatment in O_2 flow at 500 °C, the reactor bed temperature was then lowered down to room temperature by keeping the same flow rate of oxygen. Then N_2 was fed to the reactor at 30 mL/min for 1 h at room temperature to purge any residual oxygen. The catalyst was then heated to 900 °C at a constant heating rate of 10 °C/min using H_2 (5 vol%)/N_2(95 vol%) under a flow rate of 30 mL/min. H_2 concentration was monitored by the TCD detector.

2.3. Catalytic activity evaluation

The catalytic activity evaluations for the methane combustion iCMAO-800 s were carried out in a tubular plug flow reactor at atmospheric pressure. Catalysts were activated at 500 °C for 1 h in 100 mL/min air flow. After cooling down to 100 °C, a mixture of CH_4:O_2:N_2 in a volume ratio of 1:4:95 at a total flow rate of 400 mL/min passed through the catalyst bed (0.5 g catalyst diluted with similar volumed silica). The GHSV was kept approximately 50,000 h^{-1}. The system was heated externally via a tubular furnace regulated via a thermocouple inserted into the catalyst bed. The reactants and products were online analyzed by a GC equipped with FID. The column was a 60/80 Carboxen 1000 (15 ft × 1.25 in. s.s.). CO and CO_2 were

catalytically converted to CH_4 by a Ni catalyst mounted in a catalytic furnace prior to the FID measurements.

The methane conversion rate was calculated based on the integrated GC peak areas. The catalysts activity was characterized by T_{10}, T_{50}, and T_{90} representing the temperatures of methane conversion rates of 10%, 50%, and 90%, respectively. The specific activity can be characterized by the turnover frequency (TOF) of methane divided by the mass of CuO at 500 °C, i.e., μmol · m^{-2} · min^{-1} · g^{-1} CuO. It is well known that methane combustion follows a pseudo first order kinetic mechanism, so its kinetic equation could be written as ln[−ln(1−x)] = f(1000/T) [16], where x is the degree of methane conversion, and T is the Kelvin temperature at a methane conversion of x. The apparent activation energies (Ea) can be obtained from the $\ln[-\ln(1-x)]$ versus $1/T$ plots.

3. Results and discussion

3.1. Physicochemical characterization

3.1.1. X-ray diffraction analysis of iCMA-HTLCs and mixed oxides derived from HTLCs

The X-ray diffraction patterns of HTLCs (dried at 110 °C) were shown in figure 1. All the patterns show sharp and symmetric reflection at small diffraction angles, as well as weak and asymmetric reflections at larger diffraction angles, which are characteristic diffraction patterns of hydrotalcites (JCPDS 22-700). However, slight differences were observed for samples with different Cu-contents. Only hydrotalcite phases were detected in the Cu-containing 5-30CMA-HTLCs samples. In these five HTLCs catalysts, copper was incorporated into the hydrotalcite structures thoroughly and was well dispersed. However, in 40CMA-HTLC at 35.5° and 38.7°, an independent $Cu(OH)_2$ phase appeared besides the hydrotalcite. Moreover, the characteristic peaks related to (003), (006) and (009) planes become broader and move to higher 2θ with an increase in Cu content, and the peaks of (013) merged with (010) for Cu-containing samples. Further increase in copper content in CMA-HTLCs led to further broadening and weakening of the peaks of (015) and (018). Therefore, in order to obtain pure and homogeneously dispersed Cu–Mg/Al HTLCs, the CuO content in the final oxides should be controlled below 40 wt%. The weaker and broader diffraction peaks at high diffraction angles can be explained by the John–Teller effect of Cu^{2+} ion owing to its larger ionic radius in comparison with Mg^{2+} [20,21].

Figure 2 describes the XRD patterns of HTLCs after calcination at 800 °C for 5 h. The HTLC phases were completely destroyed and new oxide derivatives were formed from HTLCs. The three dominant peaks with the 2θ angle centered at 37°, 42° and 62.3° for iCMAO-800 were ascribed to periclase (MgO, JCPDS 431022). A small diffraction peak assigned to spinel phase ($MgAl_2O_4$ JCPDS 21152) appeared at 65°, whereas other peaks related to spinel could not be identified because of the interference of stronger diffractions of periclase. With increases of copper content in iCMAO-800, the diffraction intensities of peaks ascribed to periclase were reduced, but the peaks of spinel became much stronger. The stronger spinel diffractions may be caused by the superimposed $CuAl_2O_4$ inverse spinels, since their diffractions are very similar to $MgA1_2O_4$. Because of the relatively low formation temperature of $CuA1_2O_4$, the enhanced diffractions of spinels were most likely caused by the increases of $CuAl_2O_4$ spinels rather than $MgAl_2O_4$. On the other hand, the partial substitution of Mg by Cu promoted the formation of $MgAl_2O_4$ spinel too. Moreover, since the diffraction peaks of periclase and spinel phase appeared around 43°, the diffraction intensity of spinels was not weakened at a decrease of Mg^{2+} content in HTLCs, and spinel epitaxially grew along the MgO periclase surface [22].

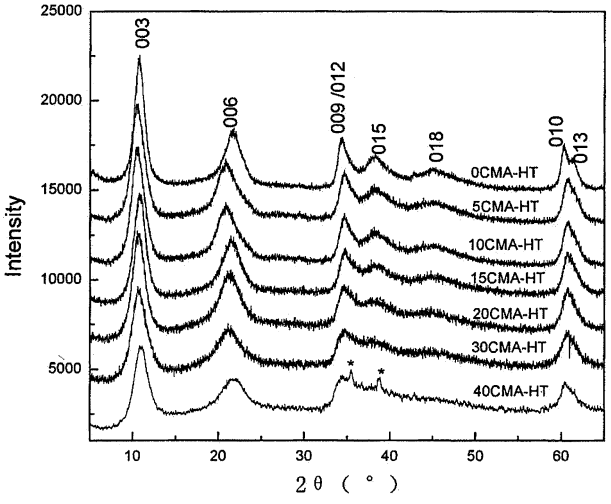

Figure 1. XRD patterns of iCMA-HTLCs (*$Cu(OH)_2$).

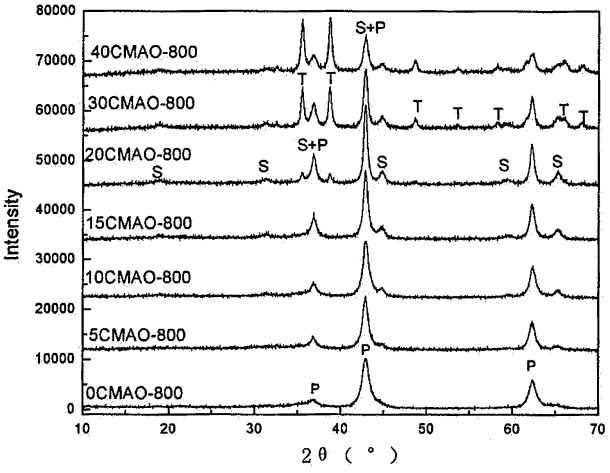

Figure 2. XRD patterns of CMAO oxides calcined at 800 °C (S = spinel, P = periclase, T = tenorite).

Table 1
Activities of CMAO catalysts calcined at 800 °C for 5 h

Samples	T_{10} (°C)	T_{50} (°C)	T_{90} (°C)	SSA (m^2/g)	TOF[a]	TOF[b] /CuO	E_a^c (KJ/mol)
Silica	925	–	950	–	0	–	285
0CMAO	628	742	803	138	0.06	–	194
5CMAO	513	591	686	125	0.21	2.12	113
10CMAO	516	582	652	110	0.21	1.04	144
15CMAO	432	521	617	84	1.34	4.48	99
20CMAO	443	533	625	60	1.46	3.66	89
30CMAO	436	520	639	57	2.05	3.41	50
40CMAO	400	483	606	59	3.25	4.06	51
Pt/Al_2O_3	425	485	550	122	4.28	–	104

[a] TOF = Turnover frequency, calculation at 500 °C, $\mu mol \cdot m^{-2} \cdot min^{-1}$.
[b] TOF[b]/CuO = Turnover frequency per gram CuO, calculation at 500 °C, $\mu mol \cdot m^{-2} \cdot min^{-1} \cdot g^{-1}$ CuO.
[c] E_a calculated from methane conversion below 40%.

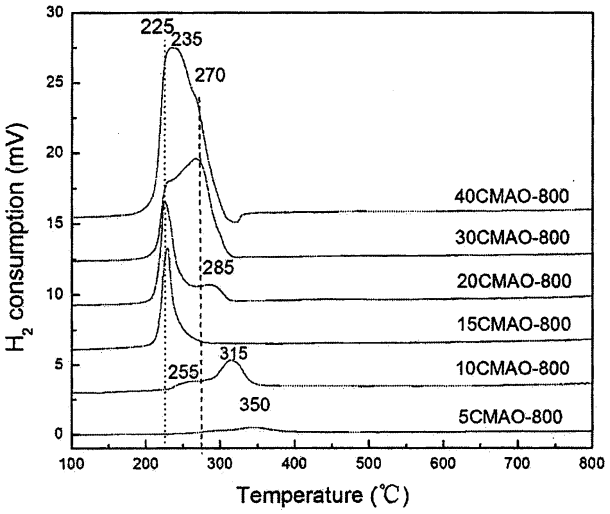

Figure 4. TPR profiles of iCMAO-800.

Another notable phenomenon is that well-crystallized CuO (tenorite) diffraction signals were detected, if copper oxide content exceeded 20 wt% in iCMA-800 catalysts. However, no teronite phases were detected, if CuO content was below 15 wt%. One possible reason was that the incorporation of copper into the MgO matrix and the formation of $CuAl_2O_4$ inverse spinel crystallites led to the high dispersion of CuO in the complex oxides. Mg^{2+} in the mixed oxides might restrict clustering and agglomeration of CuO. Because the oxides were calcined under the same conditions, the differences in diffraction patterns should result from the content of copper in precursors.

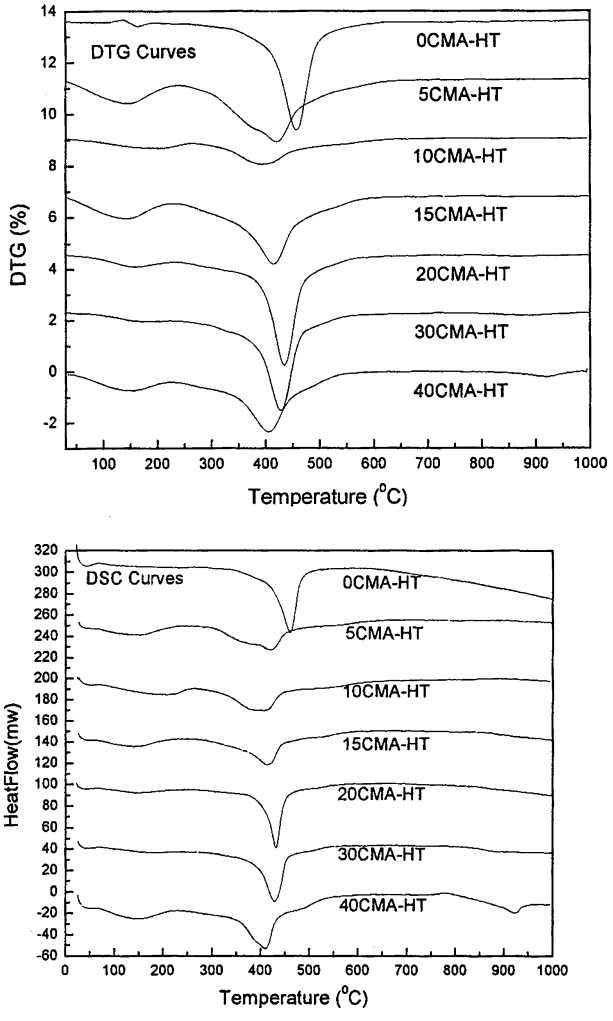

Figure 3. TG-DSC profiles of iCMA-HTLC$_s$.

3.1.2. BET areas of iCMA-800 oxides

The specific surface areas (SSA) of iCMA-800 oxides and Pt/Al_2O_3 were listed in table 1. The composition of the samples affects their SSA. The SSA changes of the mixed oxides corresponded well with their phase changes as indicated by their XRD patterns. The SSA of the mixed oxides decreased quite steadily with an increase in Cu content (as shown in figure 6) exceeding 20 wt%. At the mean time, the spinel peaks became intensified, as shown in figure 3. Consequently, an increment of Cu in hydrotalcite precursors caused a decrease of SSA in iCMAO-800, in other words, CuO in calcined oxides induced partial sintering of such samples but Mg^{2+} can depress sintering.

3.2.2. TG-DSC analysis of iCMA-HTLCs

Thermal transformation of Mg/Al hydrotalcite to oxides has been described elsewhere [23]. Generally, during calcination a typical two-stage thermal-gravity loss can be ascribed to the release of interlayer water and anions, as well as the simultaneous loss of interlayer hydroxyl groups and other anions. Elimination of hydroxyl groups was completed at higher temperatures and caused sintering of the resultant oxides. Thermal decomposition characteristics of the Cu–Mg/Al hydrotalcite-like precursors and Mg/Al-NO_3^- hydrotalcite into oxides are compared in figure 3. The two-stage weight

loss and the corresponding heat absorption of all HTCLs except 40CMA-HTLCs are shown in these DTG and DSC profiles respectively. The interlayer water released at 150–250 °C, and the temperature for water loss lowered as their copper content increased. In the course of subsequent heating at 300–550 °C, hydroxyl and nitrate groups were simultaneously transformed into water and NO_x, and the layered structures of hydrotalcites collapsed. A disordered MgO periclase phase was formed then predominantly. High Cu content (above 30 wt%) caused the formation of new mixed phases (CuO phases) after calcination around 500 °C, as shown in their XRD patterns [24]. Similar to the release of interlayer water, with an increase in the copper content of precursors, the second-stage decomposition temperature became lower and the temperature range broader. No DTG and DSC signals were detected during heating at 800–950 °C for 0–30CMA-HTLCs, and these temperature ranges were related to the phase transitions from HTLCs to spinels. The evidence of CuO decomposition in 40CMA-HT was its weight loss and heat release at 900 °C. The separated CuO phase in CMAO oxides was not stable as compared with the highly dispersed copper in the catalyst crystal structures. These findings are fairly consistent with A. Alejandre's conclusion on the decomposition of Cu/Al-hydrotalcite, who ascribed this weight loss to the transition of CuO to the more stable Cu_2O at elevated temperatures [21]. It can be conclude that an appropriate copper content (15 wt% of CuO) is a key factor for the development of stable and good Cu-containing iCMAO-800 oxide catalysts.

3.1.3. TPR analysis of iCMAO-800 catalysts

Results of temperature-programmed reduction were shown in figure 4. Different reduction behaviors could be observed depending on copper contents in oxides, except the sample OCMAO-800 which was not shown in figure 4. Kovanda *et al.* [25] detected a prevailing peak around 700 °C, which was assigned by the authors to the reduction of trace impurities in raw material [25]. Inconsistency in results of different authors might stem from different precursors selected and different purities of the Mg/Al oxide used. With an increase of copper content in HTLC precursors, several superimposed and relatively intense peaks appeared, and the reduction temperature gradually shifted to a lower range, but the extent of reduction significantly enhanced. There was only one diffuse H_2 consumption peak centered at 350 °C for 5CMAO-800, initialed at 230 °C and ended around 390 °C, which is higher than that of the bulk CuO reduction. This peak could be ascribed to the highly dispersed Cu^{2+} in bulk periclase or copper aluminate structure, because the strong affinity of CuO and supports resulted in higher reduction temperature [26]. For the sample 10CMAO-800, the two peaks centered at 255 and 315 °C corresponded to highly dispersed copper ions in the supported catalysts and in the bulk copper aluminates, respectively [21]. For the 15CMAO-800, the reduction behavior was quite different from others, and an intense and steep peak centered at 228 °C was observed. The low-temperature (225 °C) reduction characteristics of 20–40CMAO-800 samples were very similar to 15CMAO-800, except the satellite peak at 285 °C for 20CMAO-800 associated with the isolated copper oxide particulate on periclase and spinels. The broad overlapping peaks shown between 200 and 300 °C for 30CMAO-800 and 40CMAO-800 samples can be disintegrated into three peaks centered at 225, 235 and 270 °C, respectively. The peaks at 225 and 235 °C can be assigned to highly dispersed CuO particles supported on the surface of periclase and $CuAl_2O_4$ spinel. According to Severino *et al.* [27] the reducibility of surface copper aluminate was lower than that of copper oxide, and the reduction of copper aluminates takes place in the range of 230–270 °C. Thus, the last peak at 270 °C may be attributed to the reduction of the bulk CuO in the mixed oxides [26]. Although the extent of reduction of 15CMAO-800 was lower than that of 20–40CMAO-800, its H_2 consumption peak was steeper, implying the rapid reduction of copper ions. In other words, the specific activity per unit copper ion in 15CMAO-800 was comparative to the later.

3.2. Catalytic activity of methane combustion on iCMAO-800 catalysts

In the conventional Cu catalysts, alumina is usually used as the catalyst support. Over 700 °C, evaporation of CuO and interaction between copper and alumina occur, leading to partial deactivation. Alternative support material can eliminate copper-support interaction. For example, P. Artizzu *et al.* [18] have improved methane combustion by using a mangnesium aluminate support for the CuO catalysts. However, it could not prevent

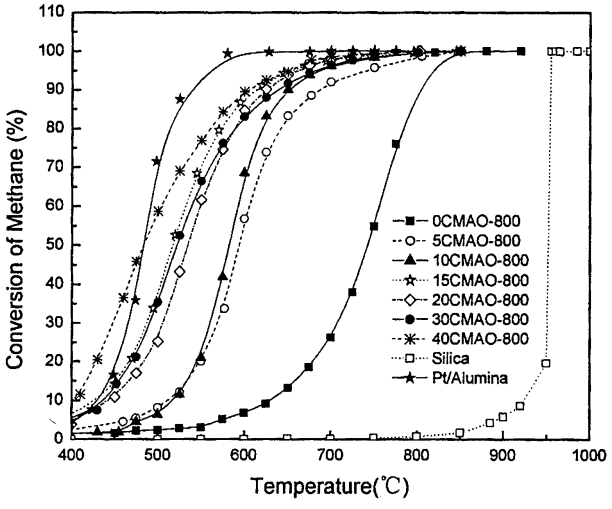

Figure 5. Temperature dependence of methane conversion on iCMAO-800.

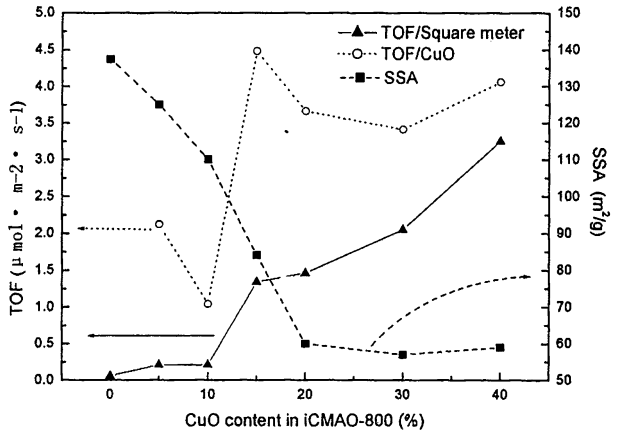

Figure 6. The effect of the CuO contents on the specific surface area (SSA) and specific activities of iCMAO-800.

evaporation of copper at elevated temperatures. Oxides derived from Cu–Mg/Al hydrotalcite may satisfy this stability requirement, since copper exists in the bulk of mixed oxides as copper aluminate.

The performance of iCMAO-800 catalysts for methane combustion was compared with that of non-catalytic thermal combustion of methane. As showed in figure 5, the conversion rate of methane can be enhanced by increase the reaction temperature. Judging from the characteristic activity data listed in table 1, incorporation of Cu into the catalysts greatly improved its activity for methane combustion, and the activity improvement depends upon the copper content. Furthermore, the light-off activities of copper-rich catalysts were comparable to the conventional Pt/alumina catalyst, though their total conversion temperatures were higher than that of Pt/alumina. In spite of the decrease in surface area with increase of the copper content, the light-off activity for methane combustion has been improved, i.e., the T_{10} decreased with increasing Cu content of iCMAO-800 catalysts. However, considering the specific activity and utility of copper for methane combustion, 15CMAO-800 was highest efficient catalyst among these catalysts. Even though 40CMAO-800 owned highest apparent activity, its lower SSA and thermal stability made it was not suitable for practical application.

No CO was detected in CH_4 combustion on iCMAO-800 ($i > 0$). However, on 0CMAO-800, the higher CO concentration 200 ppm was observed, which was produced from gas phase combustion and far lower than that (1400 ppm) on silica. The results indicated there was no thermal combustion occurred on iCMAO-800 ($i > 0$), whereas slight contribution of gas phase combustion occurred on 0CMAO-800. Generally, Mg^{2+} and Al^{3+} are all inactive for methane combustion, but methane combustion on 0CMA-800 was complete around 800 °C after light-off at 630 °C, which significantly differed from methane thermal combustion on silica, therefore, methane mainly occurred catalytic combustion on 0CMA-800. Moreover, 0CMAO-800 was much more active than $MgAl_2O_4$ for combustion as reported by P. Artizzu *et al.* [18], that methane conversion was only 30% on $MgAl_2O_4$ but over 50% on 0CMAO-800 at 750 °C. The possible reason is 0CMAO-800 catalyst having much higher SSA (110 m^2/g) than $MgAl_2O_4$ (47 m^2/g).

Although the catalytic activity of these catalysts is not directly proportional to the total amount of copper as shown in figure 6, their activities for methane combustion are reasonably related to the amount of the "reducible Cu". The appropriate copper content in the final oxides is around 15 wt%. Both TPR results and reaction data confirmed this point.

4. Conclusions

A series of Cu–Mg/Al mixed oxide catalysts derived from calcined Cu-containing hydrotalcite precursors with $M^{2+}/M^{3+} = 3$ were prepared, using co-precipitation and thermal evolution methods. TG-TSC, XRD, BET, and TPR techniques were used for catalyst characterization.

Cu was highly dispersed in hydrotalcite precursors in case of low copper contents (Cu < 40 w%). For higher Cu contents, $Cu(OH)_2$ was formed, and, consequently, a separate phase of CuO was detected in the oxide catalysts after calcination. Thermal calcination promoted the formation of copper aluminates and segregation of Cu ions from the bulk phases.

The catalytic activity for methane combustion is closely related to the copper species and Cu content in calcined oxides, and, magnesium presented in the oxides enhanced their stability though decreased their reducibility. The appropriate copper content is around 15 wt%.

Acknowledgments

Financial funds from the Chinese Natural Science Foundation (project no. 20322201). The Knowledge Innovation Funds of the Chinese Academy of Sciences (key project KZCX3-SW-430) and the Asian Regional Research Programme on Environmental Technology (ARRPET) sponsored by the Swedish International Development for Research Cooperation Agency (SIDA) are gratefully acknowledged.

References

[1] F. Cavani, F. Trifiro and A. Vaccari, Catal. Today 11 (1991) 173.
[2] J.M.L. Nieto, A. Dejoz and M.I. Vazquez, Appl. Catal. 132 (1995) 41.
[3] S. Velu and C.S. Swamy, Catal. Lett. 40 (1996) 265.
[4] M. Belloto, B. Rebours, O. Clause, J. Lynch, D. Bazin and E. Elkaim, J. Phys. Chem. 100 (1996) 8527.
[5] C. Depege, L. Bigey, C. Forano, A. de Roy and J.P. Besse, J. Solid State Chem. 126 (1996) 314.

[6] S. Velu, V. Ramaswamy, A. Ramani, B.M. Chanda and S. Sivasanker, Chem. Commun. (1997) 2107.
[7] S. Velu, K. Suzuki, T. osaki, F. Ohashi and S. Tomura, Mater. Res. Bull. 34 (1999) 1707.
[8] U.P. Pillai and E. Sahle-Demessie, J. Mol. Catal. A 191 (2003) 93.
[9] S. Velu, K. Suzuki and T. Osaki, Chem. Commun. (1999) 2341.
[10] S. Velu and K. Suzuki, J. Phys. Chem. B. 106 (2002) 12737.
[11] L. Chmielarz, P. Klustrowski, A.R. Lasocha and R. Dziembaj, Appl.Catal. B 35 (2002) 195.
[12] M. Trombetta, Langmuir 13 (1997) 4628.
[13] L. Pfefferle and W. Pfefferle, Catal. Rev. 29 (1987) 219.
[14] P.O. Thevenin, A.G. Ersson, H.M.J. Kusar, P.G. Menon and S.G. Jaras, Appl. Catal. A 212 (2001) 189.
[15] Jon G. McCarty, Nature 403 (2000) 35.
[16] P. Forzatti and G. Groppi, Catal. Today 54 (1999) 165.
[17] P. Artizzu, N. Guilhaurne, E. Garbowski, Y. Brull'e and M. Primet, Catal. Lett. 51 (1998) 69.
[18] P. Artizzu, E. Garbowski, M. Primet, Y. Brulle and J. Saint-Just, Catal. Today 47 (1999) 83.
[19] V.C. Belessi, A.K. Ladvos and P.J. Pomonis, Appl. Catal. B 31 (2001) 183.
[20] W.T. Reichle, Solid State Ionics 22 (1986) 135.
[21] A. Alejandre, F. Medina, P. Salagre, X. Correig and J.E. Sueiras, Chem. Mater. 11 (1999) 939.
[22] S. Narayanan and K. Krishna, Chem.Commun. (1997) 1991.
[23] M. Bellotto, B. Rebours, O. Clause, J. Lynch, D.E. Bazin and Elkaim, J. Phys.Chem. 100 (1996) 8535.
[24] J.J. Yu, Z. Jiang, Z.P. Hao, S.F. Kang and C. Hu, Chin. Chem. phys. (2004) Accepted.
[25] F. Kovanda, K. Jiratova, J. Rymes and D. Kolousek, Appl. Clay Sci. 18 (200l) 71.
[26] K.T. Jacob and C.B. Alcock, J. Am. Ceram. Soc. 38 (1975) 192.
[27] F. Severino, J. Brito and J. Laine, et al. J. Catal. 102 (1986) 172.